Published in final edited form as:
Biomed Microdevices. 2012 April ; 14(2): 419–426. doi:10.1007/s10544-011-9618-3.

Systematic Prevention of Bubble Formation and Accumulation for Long-Term Culture of Pancreatic Islet Cells in Microfluidic Device

Yong Wang[a,*], **Dongyoung Lee**[a,b,*], **Lisa Zhang**[a], **Hyojin Jeon**[a], **Joshua E. Mendoza-Elias**[a,b], **Tricia A. Harvat**[a], **Sarah Z. Hassan**[a], **Amanda Zhou**[a], **David T. Eddington**[b], and **José Oberholzer**[a,b,**]

[a]Department of Transplant/Surgery, University of Illinois at Chicago, IL, USA

[b]Department of Bioengineering, University of Illinois at Chicago, IL, USA

Abstract

Reliable long-term cell culture in microfluidic system is limited by air bubble formation and accumulation. In this study, we developed a bubble removal system capable of both trapping and discharging air bubbles in a consistent and reliable manner. Combined with PDMS (Polydimethylsiloxane) hydrophilic surface treatment and vacuum filling, a microfluidic perifusion system equipped with the bubble trap was successfully applied for long-term culture of mouse pancreatic islets with no bubble formation and no flow interruption. In addition to demonstrating normal cell viability and islet morphology, post-cultured islets exhibited normal insulin secretion kinetics, intracellular calcium signaling, and changes in mitochondrial potentials in response to glucose challenge. This design could be easily adapted by other microfluidic systems due to its simple design, ease of fabrication, and portability.

Keywords

Microfluidics; Air Bubble; Bubble Trap; Islets of Langerhans; β-cells; Cell Culture

1. Introduction

Bubble formation and accumulation is a critical obstacle in microfluidic applications, especially when long-term cell culture is involved. Within a microfluidic device, air bubbles have the tendency to arise both occasionally and continuously due to factors such as: changes in temperature, channel geometry, hydrophobic properties of PDMS, flow-focusing; and lastly from configurations of connectors, adaptors, and valves. All of these factors play a significant role in bubble formation and accumulation (El-Ali et al., 2005; Gordillo et al., 2005; Prakash et al., 2007; Xu et al., 2008). In the microfluidic environment, unfortunately once an air bubble forms it is extremely difficult to remove. Undesired bubbles are also associated with abrupt changes in flow dynamics and channel clogging, resulting in impaired performance of the microfluidic device. Additionally, air bubbles can result in cell damage and even death when the surface tension of the air-liquid interface is large enough to rupture cell membranes. Therefore, the development of a bubble trap that is capable of

**Corresponding author: José Oberholzer, M.D., jober@uic.edu, University of Illinois at Chicago, Department of Transplant/Surgery, 840 South Wood Street, Clinical Sciences Building, Suite 402, Chicago, Illinois 60612. jober@uic.edu, Phone: +1 312 996 6771, Fax: +1 312 413 3483.
*Equal contribution: Yong Wang and Dongyoung Lee

removing unwanted bubbles will prove worthwhile, especially for applications requiring long-term constant flow.

One of the research applications that would be benefit with a bubble trap is the microfluidic-long-term culture of pancreatic islets. *In vivo*, pancreatic islets of Langerhans are exposed to dynamic microenvironments and secrete hormones in response to blood glucose level changes via rapid modulation of cell energetics, metabolic activities, and ion cascades. With this in mind, microfluidic technology has a distinct advantage in studying β-cell physiology *in vitro*. Microfluidic technology exhibits the ability to intently emulate *in vivo* islet microenvironments with greater precision and flexibility of flow control (Dishinger et al., 2007; Easley et al., 2009; Mohammed et al., 2009; Roper et al., 2003; Shackman et al., 2005) when compared to either static or macroperfusion cell culture systems. The principles governing the design, fabrication, and application of microfluidics for islet research have been previously described and are actively pursued (Wang et al., 2010); however, most of these studies focus on short-term applications, such as islet hormone secretion and regulation in response to stimuli. Currently, microfluidic long-term islet culture has not been thoroughly investigated and developed, in part due to easy formation and accumulation of air bubbles in the device over time.

Various stand-alone or integrated (on-line) bubble trapping systems have been investigated in the past to address this problem (Kang et al., 2008; Skelley et al., 2008; Sung et al., 2009). While some bubble trap methods have demonstrated practicality for a given application, each system has its own limitation(s) including: flow interruption, needs for external pressures or vacuums, complex fabrication, and setup expertise. Recently, a simple and effective bubble trap and discharge system was developed (Zheng et al., 2010) that allowed for the bubble trap to be an integrated component of a microfluidic system with no flow interference and high flow stability. Unfortunately, the fabrication process for such an integrated system remained relatively complex and its design geometry presents constrain that is not easily adaptable to all types of microfluidic applications.

In this study we developed a modular bubble trap and discharge system similar in principle to the integrated bubble trap developed by Zheng et al., but with two different advantages: (i.) it is portable and bubble trap can be placed at different locations; (ii.) bubble trap geometry is not constrained by microfluidic device geometry, thereby allowing easy integration into many microfluidic devices without major configuration changes. In conjunction with comprehensive PDMS surface treatment, we were able to successfully apply long-term dynamic islet culture in a microfluidic device with minimal bubble formation and accumulation.

2. Methods and Materials

2.1 Design and fabrication of multiplexer microfluidics

For long-term islet culture, a PDMS-based multiplexer microfluidic device was designed using CAD software. As shown in diagrammatized schematics in Figure 1, based on our previous devices, the device is composed of three layers with three functionally identical and independent perifusion systems. The top layer of each perifusion system has two inlets and one outlet. In addition, a chaotic mixer, based on our previous design (Lee et al., 2011), was employed using six staggered herringbone mixers within a serpentine channel (6 mm in length) with a channel aspect ration of 0.2 ($h/w = 0.2$), a groove-to-depth ratio of 1.6 ($d/h = 1.6$), and a ridge length of 145 μm. As described previously by Stroock et al. (Stroock et al., 2002), this mixer enables solution mixing and creation of a dynamic cell culture environment through temporal chemical gradients. The middle layer was a perifusion chamber with a total chamber volume of 50 μL (height and diameter: 3 mm and 7 mm,

respectively). The bottom layer consisted of an array of microwells for islet immobilization (height and diameter: 100 μm and 350 μm, respectively). The detailed fabrication process has been described in our previous work (Adewola et al., 2010; Mohammed et al., 2009). Briefly, a 3-inch silicon wafer was sequentially cleaned with acetone, methanol and isopropanol. The wafer was then dried with nitrogen gas and further treated with oxygen plasma at 100 W for 30 s (Plasma Preen) to oxidize any residual organic molecules. SU-8 photoresist was then spin-coated on the wafer, patterned, and further developed using standard protocols. These steps were repeated for each layer. PDMS was then poured over each photoresist mold and cured at 80 °C for 120 min. The inlets and outlets were made on the cured PMDS using a 2 mm hole-punch. All of the layers were bound together using an oxygen plasma torch and further annealed on a hot plate for 2 hrs at 75 °C to form the final device.

2.2 PDMS surface treatment

Chemically, the surface of PDMS is hydrophobic, making it difficult for aqueous solutions to coat the inside of PDMS channels. As a result, bubbles tend to form when fluid is forced onto hydrophobic PDMS surfaces. In addition, microscopic bubbles can be easily trapped in between the PDMS layers of a microfluidic device due to the uneven and incompleteness of PDMS bonding. In this study, we modified a previously described approach for bubble formation prevention and entrapment via a combination of hydrophilic surface treatment and a vacuum filling method (Monahan et al., 2001). Our method is a five-step process: (i.) the microfluidic device was first immersed in a vessel and flushed with 100% EtOH for 10 min; (ii.) the ethanol-treated device was then placed into a Pyrex brand vacuum desiccator (Fisher Scientific, PA) connected to a standard laboratory wall vacuum system for 30 min at a pressure of ~110–120 kPa; (iii.) 100% EtOH was then exchanged with distilled (DI) water; (iv.) and vacuum treated for an additional 30 min; (v.) the device was removed from the desiccator, wrapped in foil, and autoclaved at a temperature of 125 °C for 30 min. A schematic of the chemical surface treatment is shown in Figure 2.

To test the efficacy of the PDMS surface treatment in preventing bubble formation and accumulation in the microfluidic device, both treated and untreated islet perifusion chambers were perifused with a RPMI 1640 cultured medium containing 10% Fetal Bovine Serum (FBS) at a constant flow rate of 25 μL/min under 37°C, and microscopically monitored over a 24-hr period.

2.3 Design and fabrication of the bubble trap

In this study, a simple portable ad-hoc bubble trap was designed for both trapping and discharging of air bubbles. The design was based on the principles of an IV drip chamber that allows air to rise out from a fluid surface and air accumulated overtime may be discharged from release valve on top or via bypass tubing (Figure 3). The detailed experimental setups will be discussed in a later section.

The bubble trap is a three-layer PDMS structure with a simple fabrication process. To briefly summarize, two PDMS sheets with a thickness of 0.5 cm (for the top and bottom layers) and 1.0 cm PDMS sheet (for the middle layer) were first casted. The middle layer was then hole-punched with two 8 mm hole-punches to create two cylindrical chambers. The cylindrical dimensions might be varied based on inlet geometry of microfluidic device and could be customarily designed according to experimental needs. Each cylindrical chamber was identical and had a height of 1.0 cm, a diameter of 0.5 cm, with a total liquid volume of 196 μL. Flow inlets were punched perpendicular to each cylindrical chamber using a 2.0 mm hole-punch. The top layer consisted of air bubble release holes; also punched using the same 2.0 mm hole punch. In the same fashion, an outflow outlet was

created on the bottom layer of the bubble trap. After all the layers were punched, they were corona treated with an oxygen plasma torch and further annealed at 80 °C for 2 hrs.

2.4 Islet isolation

Mouse pancreatic islets were isolated from the pancreata of 10–12 week-old C57/B6 mice (Jackson Laboratory, MA) and cultured according to standard protocol. In brief, the pancreata were injected with 0.375 mg/mL of Collagenase P (Roche Applied Science, IN) in a retrograde manner through the pancreatic duct. The distended pancreata were removed and incubated at 37 °C for 15 min. The digested pancreata were then shaken vigorously by hand for 5 s to dissociate pancreatic acinar tissue. The digested tissues were washed with HBSS twice and islets were then separated from acinar tissues by centrifugation through a discontinuous Ficoll gradient (Mediatech, VA). Finally, the islets were cultured in RPMI 1640 medium supplemented with 10% fetal bovine serum (Hyclone Inc., MA) and 1% penicillin/streptomycin at 5% CO_2 at 37 °C.

2.5 Bubble system setup and long-term islet culture

Figure 3 shows the assembled system for long-term islet culture including the multiplex microfluidic device and the bubble trap. Initially, all ports of the bubble trap were inserted with 1/16 inch barbed connectors. The bubble trap was then connected to the microfluidic device inlet ports. Next using silicone tubing, two side ports were connected to two 140 mL syringes driven by syringe pumps (model 200; Harvard apparatus, MA). One syringe pump delivered RPMI 1640 culture medium and the other delivered insulin secretagogues (such as high glucose solution), to test insulin release capabilities of the islets in response to a challenge.

The bubble trap was setup experimentally in two different ways. In configuration A (Figure 3a), the releasing port of the bubble trap was directly connected to a 0.22 μm filter. The installed filter allowed for free exchange of air with ambient environment while maintaining sterility. In addition, the open nature of the system prevents accumulation of air pressure caused by trapped bubbles inside the bubble trap while avoiding uncontrolled emptying of the device caused by accumulated pressure changes. Since both hydrostatic pressures of the fluid reservoir and the perifusate collector will influence the hydrostatic pressure generated inside the modular trap, meticulous adjustment of liquid levels maintaining an equivalent level is crucial in avoiding spillage of perifusing media over the air filter and subsequent liquid drainage from the bubble trap into the chaotic mixer and perifusion chamber.

In configuration B (Figure 3b), the releasing port of the bubble trap was first connected with silicone bypass tubing and then to a 0.22 μm filter. For unmonitored long-term cell culture, hydrostatic pressure is often increased in the perifusate collector overtime due to fluid accumulation. Such pressure changes will influence backpressure of the outlet and may subsequently cause spillage of the perifusing medium onto the filter thus compromising sterility and pressure releasing functions. The bypass tubing was intended to prevent such accidental overflow of medium.

To verify and characterize the effectiveness of our bubble trapping and discharge system, we initially cultured mouse islets in the multiplex microfluidic device using modular trap configuration B over a 24-hr period. After overnight post-isolation culture, ten mouse islets were handpicked under a microscope and transferred into the device via loading port. The islets were cultured under dynamic conditions via a syringe pump containing RPMI 1640 at a speed of 25 μL/min in an incubator at 37 °C and 5% CO_2 for 24 hrs. Post-culture islet viability and functionality were further verified as described below.

2.6 Simultaneous fluorescence imaging of intracellular calcium and mitochondrial potentials

For post-culture fluorescence imaging experiments, the microfluidic device containing the long-term cultured islets were flushed with Krebs-Ringer Buffer (KRB) containing 2 mM glucose (KRB2) for 30 min at a speed of 500 μL/min followed by fluourescence labeling with 5 μM Fura-2/AM (Fura-2, a calcium indicator; Molecular Probes, CA) and 2.5 μM Rhodamine 123 (Rh123, a mitochondrial potentials indicator: Sigma, MO) statically for 30 min at 37 °C and 5% CO_2. The microfluidic device was then mounted on an inverted epifluorescence microscope (Leica DMI 4000B, IL). The fluorescently labeled loaded islets were then washed with continuous flow of KRB2 at 37 °C (pH 7.4) for 10 min. 14 mM glucose KRB (KRB14) was then administered to the islets using a syringe pump at a speed of 500 μL/min. Dual-wavelength Fura-2AM was excited at 340 and 380 nm and fluorescent emission was detected at 510 nm. Increases in intracellular calcium concentration ($[Ca^{2+}]_c$) were expressed as a ratio of emission intensity F_{340}/F_{380} (%). Rh123 is a lipophilic cation that partitions selectively into negatively-charged mitochondrial membranes. Glucose-induced hyperpolarization of the mitochondrial membrane causes increased uptake of Rh123 into the mitochondria with a subsequent decrease in Rh123 fluorescence due to intermolecular crowding mediated fluorescence quenching, resulting in a detectable loss in signal. Rh123 was excited at 490 nm, and emission was measured at 530 nm. Fura-2 and Rh123 fluorescence emission spectra were filtered using a Fura-2/FITC polychroic beamsplitter and double band emission filter (Part number: 73100bs; Chroma Technology, VT) and these images were collected with a CCD (Retiga-SRV, Fast 1394; QImaging, Canada). SimplePCI software (Hamamatsu Corp, NJ) was used for image acquisition and analysis. Both fluorescence signals were acquired every 15s and expressed as “change-in-percentage” after being normalized against basal intensity levels established before stimulation. A fraction collector was used to collect the perifusates from the outlets (model 203B; Gilson, WI) at an interval of 500 μL/min to determine β-cell insulin secretory kinetics using an ELISA kit (Mercodia AB, Sweden) according to the manufacturer recommended protocol.

2.7 Cell viability assay

Post-culture islet viability was determined using inclusive and exclusive fluorescent staining with Syto-Green (Life technology, NY) for live cells and Ethidium bromide (Sigma, MO) for dead cells, as previously described (Ricordi et al., 1990).

3. Results and discussion

3.1 Evaluation of PDMS surface treatment efficacy

As shown in Figure 4a, some small bubbles were observed in the untreated perifusion chamber after 2 hrs. From 4 to 24 hrs, more bubbles appeared and eventually all small bubbles coalesced into several large bubbles. However, in the pre-treated device, the PDMS surface had no bubble formation over a 24-hr period (Figure 4b). As previously indicated, the lifetime of PDMS surface hydrophilicity treatment with either plasma or ethanol is limited to only a few hours, and bubbles can still form overtime. Our experience demonstrated a similar result (data not shown). Unlike the single channel device, our perifusion chamber (used for long-term culture of multiple islets) had a larger surface area that was more likely to form and trap bubbles once they formed inside the perifusion chamber. Recently, Monahan et al. reported a vacuum filling method that was shown to be more effective than hydrophilic surface treatment (Monahan et al., 2001). In this study, we integrated the hydrophilic surface treatment with the proposed simplified vacuum filling method. Using a conventional laboratory vacuum, we successfully demonstrated that a long-time bubble-free system was possible.

3.2 Evaluation of the modular trap efficiency

After the bubble trap was integrated with the microfluidic device, the system was loaded with 1% blue food dye (vol/vol) and the efficacy of the modular trap for trapping and discharging air bubbles was tested for each configuration by deliberately introducing various sizes of air bubbles at flow speeds ranging from 50–1000 μL/min.

In testing configuration A, the fluid level of the flow reservoir was first carefully adjusted to be the same as that of the perifusate collector. Then the colored liquid containing deliberately introduced air bubbles was delivered through the inlet tube at a speed of 250 μL/min. The results demonstrated an efficient capability of air bubble trapping by the modular trap (Supplement 1: Movie Clip 1, MC1). The void space occupied by the bubbles in the modular trap had free exchange with air via the 0.22 μm air filter; therefore, the fluid level in the modular trap was kept relatively stable without any overflow or drainage of the bubble trap liquid into the perifusion chamber. Next, hydrostatic pressure in the perifusate collector was manually adjusted to be far greater than the flow reservoir via increasing the fluid height level. This caused fluid to overflow and spill into the bypass tubing and liquid to contact the 0.22 μm filter (Supplement 1: MC 2). In configuration B testing, the pump speed was increased from 250 to 500 μL/min (another way to cause overflow), the bubble trap was still able to efficiently trap bubbles and dissipate them, without obvious flow spilling or drainage (Supplement 1: MC 3). It should be noted that the minimum height of the bypass tubing should be made to be below height level of the flow reservoir, therefore allowing pressure to predominate over tubing length in flow resistance.

Furthermore, integrated with the bubble trap and comprehensive PDMS surface pretreatment, the microfluidic device was maintained bubble-free over a 72 hr period when perifused with RPMI 1640 culture medium supplemented with 10% FBS at flow rate of 25 μL/min at 37 °C (data not shown).

3.3 Outcomes of long-term dynamic islet culture in microfluidics

Comparable to static-cultured islets, dynamic, post-dynamically cultured islets were shown to have normal morphology and viability (Figure 5a, b, and c) using inclusion and exclusion dyes (static: 96.5 % ± 2.1 and microfluidic dynamic: 97.3 ± 1.6; $p = 0.45$ tested by a paired student *t*-test). There were few, if any, individual cells protruding from the smooth rounded surface and any obvious hypoxic-induced necrotic cells in the center of the islets were not observed.

We further tested post-cultured islet function and viability by measuring glucose-induced calcium influx, changes in mitochondrial potentials ($\Delta\Psi_m$), and insulin secretion kinetics. β-cell insulin secretion in response to glucose stimulation is governed by cellular electrical activity, metabolic events, and ion signaling, which display complex biphasic and pulsatile kinetic profiles. Glucose-induced insulin secretion is a dynamic process and tightly regulated. In short, glucose enters β-cells via the GLUT2 transporter and then undergoes glycolysis in the cytoplasm. Pyruvate generated in glycolysis enters the Tricarboxylic Acid Cycle (TCA cycle) in the mitochondria and produces NADH which then enters the electron transport chain and generates an electric potential gradient across the mitochondrial membrane. The mitochondrial hyperpolarization subsequently leads to ATP generation and closure of ATP-sensitive K^+ (K_{ATP}) channels, initiating plasma membrane depolarization and an increase in $[Ca^{2+}]_i$ through the rapid influx of calcium ions via voltage-dependent calcium channels (VDCCs). This glucose-induced increase in $[Ca^{2+}]_i$ further triggers the fusion of the insulin granules with the cell membrane and the exocytosis of insulin (Henquin et al., 2006)

Our results showed that dynamically cultured islets had a normal physiological response to glucose challenge, starting with mitochondrial hyperpolarization and then biphasic intracellular calcium signaling accompanied with second phase slow calcium oscillations indicating islet function (Figure 6a). Finally, a typical biphasic secretion of insulin was observed (Figure 6b).

4. Conclusion

PDMS-based microfluidic devices have many advantages for live-cell research, including: biocompatibility, inexpensive rapid fabrication, and high gas permeability. In this study, we designed a portable bubble trap and discharge system that demonstrated the ability to confine air bubbles delivered upstream of the bubble trap with no flow interference and good flow stability. The portable bubble trap has a simple geometry and is easy to fabricate and customize to a specific microfluidic device. In addition, the PDMS surface treatment prior to islet culture can help limit bubble formation and generation in the perifusion chamber. More importantly, we demonstrated that the presence of a bubble trap enhanced the operation of the microfluidic device in continuous long-term islet culture without interruption, disconnection or reconnection during culture periods. These results are encouraging for the islet community seeking long-term dynamic culture of islets, as well as any long-term culture of cell related tissue engineering and cell analysis applications that utilize PDMS-based microfluidics.

Supplementary Material

Refer to Web version on PubMed Central for supplementary material.

Acknowledgments

This work was supported in part by the **NIH R01 DK091526** (JO, YW, and DE) and a startup grant by the **University of Illinois at Chicago College of Medicine** (J.O) and the **Chicago Diabetes Project** (CDP). We would also like to thank the CDP summer internship students who played a role in this study: Laura Gotaas, Weston Terrasse, Daniela Girotti, Jason Ross, and Amanda Zhou.

References

Adewola AF, Lee D, et al. Biomed Microdevices. 2010; 12
Dishinger JF, Kennedy RT. Anal Chem. 2007; 79
Easley CJ, Rocheleau JV, et al. Anal Chem. 2009; 81
El-Ali J, Gaudet S, et al. Anal Chem. 2005; 77
Gordillo JM, Sevilla A, et al. Phys Rev Lett. 2005; 95
Henquin JC, Nenquin M, et al. Diabetes. 2006; 55
Kang JH, Kim YC, et al. Lab Chip. 2008; 8
Lee D, Wang Y, et al. Biomed Microdevices. 2011
Mohammed JS, Wang Y, et al. Lab Chip. 2009; 9
Monahan J, Gewirth AA, et al. Anal Chem. 2001; 73
Prakash M, Gershenfeld N. Science. 2007; 315
Ricordi C, Gray DW, et al. Acta Diabetol Lat. 1990; 27
Roper MG, Shackman JG, et al. Anal Chem. 2003; 75
Shackman JG, Dahlgren GM, et al. Lab Chip. 2005; 5
Skelley AM, Voldman J. Lab Chip. 2008; 8
Stroock AD, Dertinger SK, et al. Science. 2002; 295
Sung JH, Shuler ML. Biomed Microdevices. 2009; 11
Wang Y, Lo JF, et al. Bioanalysis. 2010; 2

Xu JH, Li SW, et al. Langmuir. 2008; 24
Zheng W, Wang Z, et al. Lab Chip. 2010; 10

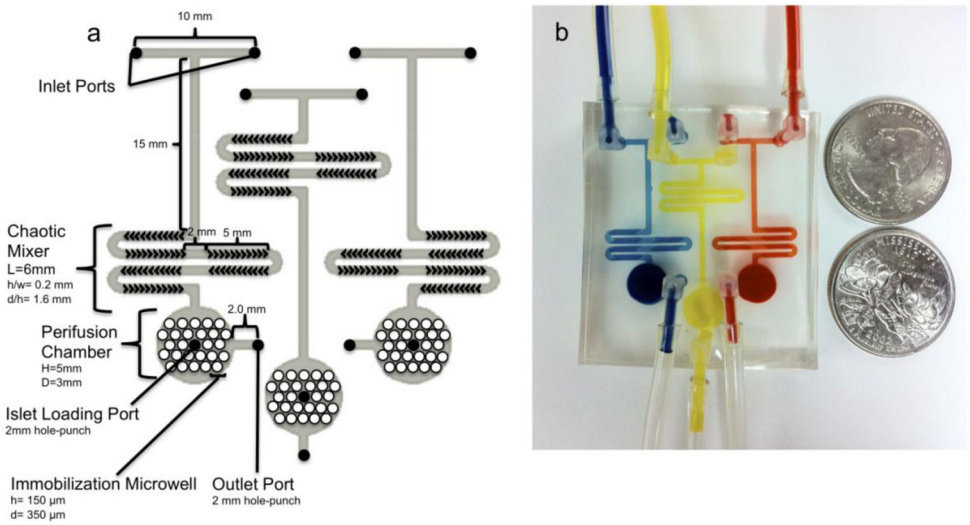

Figure 1. Multiplex microfluidic device for long-term islet culture

(**a**) Schematic diagram of the multiplex perifusion network. (**b**) A picture of the perifusion multiplex device for long-term islet culture with three functionally identical perifusion chambers. For each microfluidic network, the top layer contains two inlets, a chaotic mixer, and one outlet. The middle layer is a perifusion chamber with a total volume of 50 μL. The bottom layer has an array of microwells (350 μm in diameter and 100 μm in depth) for islet immobilization.

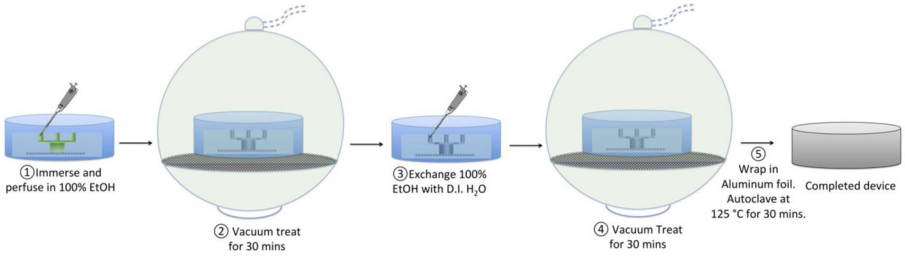

Figure 2. Schematic diagrams of PDMS surface treatment and vacuum filling

Detailed five steps of PDMS surface treatment and vacuum filling protocol in prevention of bubble formation and accumulation.

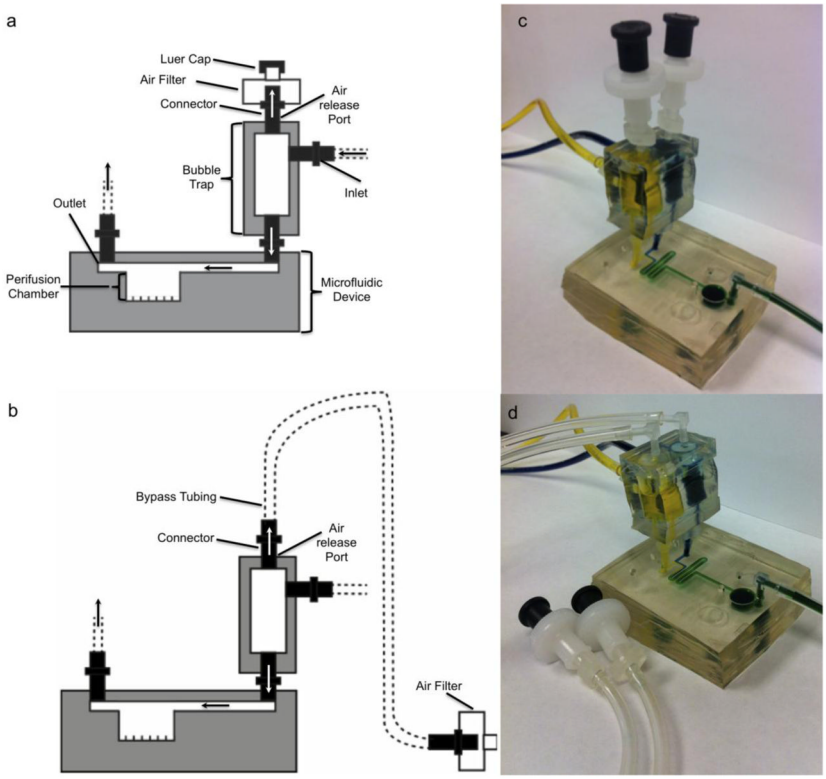

Figure 3. The modular trap design and setup

(**a and c**) Schematic diagram and picture of the modular trap design and experimental setup for configuration A with the multiplexer microfluidic device. (**b and d**) Schematic diagram of the modular trap design and experimental setup for configuration B with the multiplexer microfluidic device. The following description is for each microfluidic perifusion system. The top layer of the modular trap has two air release outlets connecting either a 0.22 μm air filters capped with or without a luer cap or bypass tubing capped with a 0.22 μm air filter. The middle layer has a volume of 194 μL for trapping upstream bubbles with two inlets feeding in perifusing media. The bottom layer has two outlets connecting the modular trap with the microfluidic perifusion device flow inlet.

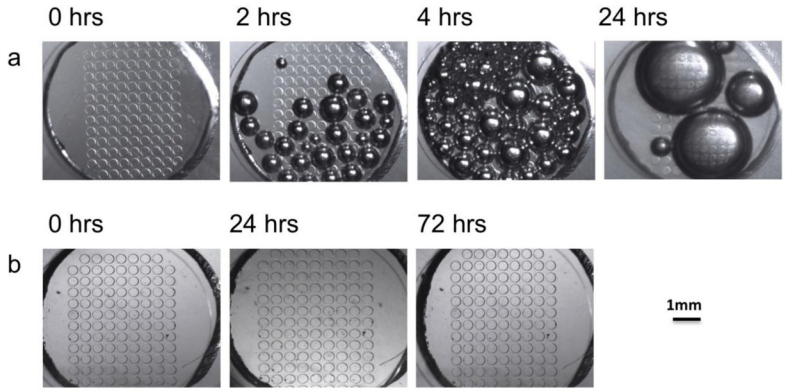

Figure 4. Evaluation of PDMS surface treatment efficacy without the bubble trap

(**a**) Bright field microscopy images of the perifusion chamber without surface treatment over a 24 hr period of perfusion at a speed of 25 μL/min. (**b**) Bright field microscopy images of the surfaced treated perifusion chamber over a 72 hr period of perfusion at 25 μL/min. Scale bar is 1 mm.

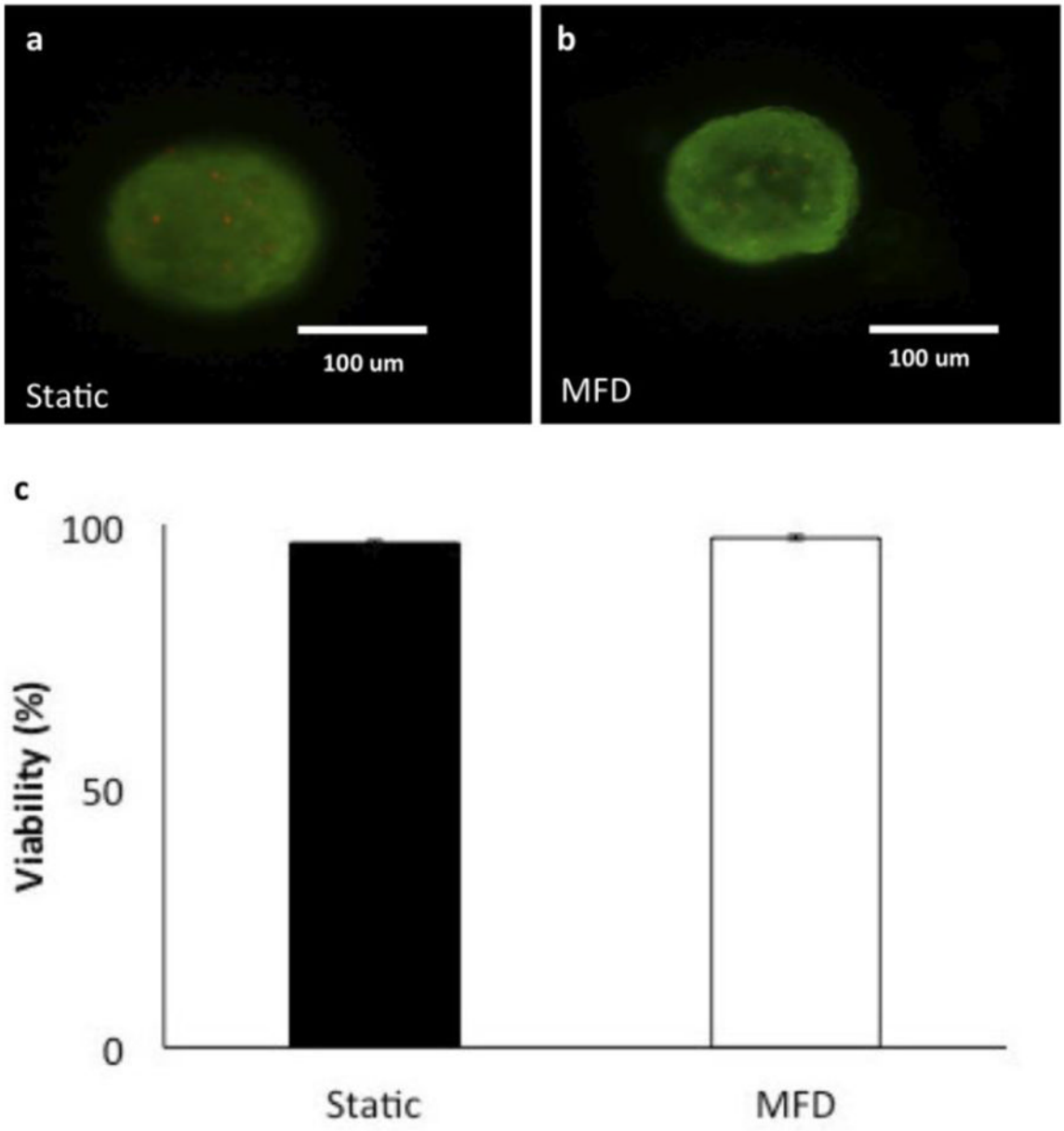

Figure 5. Evaluation of post-culture islet viability

(a) Viability staining of islets under static culture after 24 hrs. (**b**) Viability staining of the islets undergoing dynamic culture after continuous perfusion for 24 hrs at a rate of 25 μL/min. Green fluorescence (Syto-green) indicates live cells and red (Ethidium bromide) indicates dead cells. Scale bar is 100 μm. (**c**) Quantified cell viabilities of both static and dynamically cultured islets (n =7 each, $p = 0.45$)

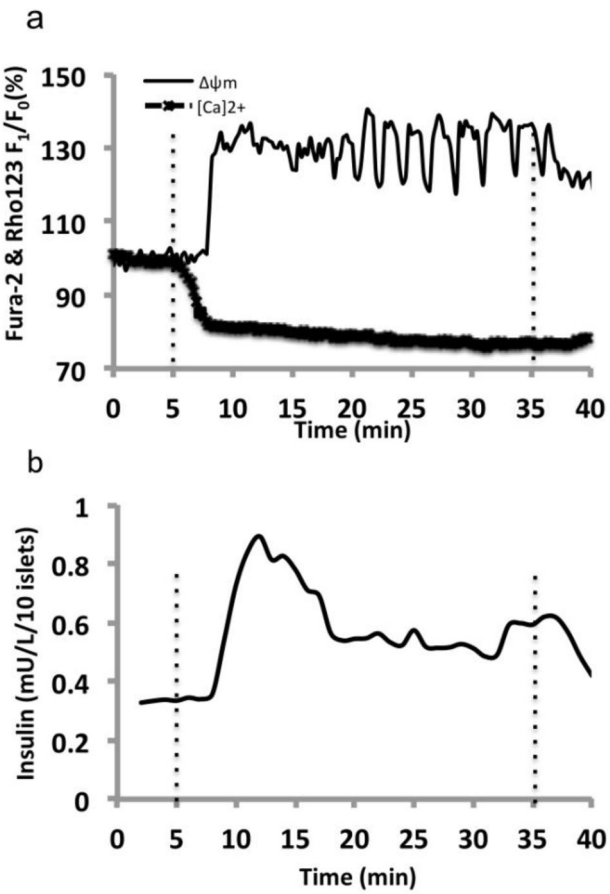

Figure 6. Simultaneous islet perifusion and multi-channel fluorescence imaging of dynamic post-cultured islets in response to 14 mM glucose

(**a**) A representative fluorescence intensity plot of $[Ca^{2+}]_c$ (intracellular calcium concentration) and $\Delta\Psi_m$ (mitochondrial potentials) of post-cultured islets in response to stimulation with 14 mM glucose (n =10 islets). The fluorescence signals were normalized against basal intensity, established before glucose stimulation and expressed in percentage change. (**b**) A representative trace of the insulin secretory kinetics from 10 post-cultured islets in response to 14 mM glucose. Flow rate of 14 mM glucose delivered was at rate of 250 μL/min. Dotted lines indicate when stimulation arrived and left the perifusion chamber.